arXiv:1512.08950v3 [hep-th] 18 Jun 2016

A general holographic insulator/superconductor model away from the probe limit

Yan Peng[1,2*]
[1] *School of Mathematical Sciences, Qufu Normal University, Qufu, Shandong 273165, China and*
[2] *School of Mathematics and Computer Science, Shaanxi Sci-Tech University, Hanzhong, Shaanxi 723000, China*

Qiyuan Pan[3†]
[3] *Department of Physics, Key Laboratory of Low Dimensional Quantum Structures and Quantum Control of Ministry of Education, Hunan Normal University, Changsha, Hunan 410081, China*

Yunqi Liu[4‡]
[4] *School of Physics, Huazhong University of Science and Technology, Wuhan, Hubei 430074, China*

Abstract

We investigate holographic phase transitions affected by dark matter sector in the AdS soliton background away from the probe limit. When neglecting backreaction, the scalar charge q can be scaled unity without loss of generality. While considering backreaction in this work, we obtain much more richer physics by choosing various scalar charge q. Firstly, we observe unstable retrograde condensation appears due to the dark matter sector and also derive stable conditions. For stable solutions, we find that the larger coupling parameter α makes the gap of condensation shallower and the critical chemical potential keeps as a constant with a large scalar charge q, which is similar to cases in the probe limit. In contrast, the dark matter sector could affect the critical chemical potential and the order of phase transitions for very small charge q. We also arrive at the same conclusion from the holographic topological entanglement entropy approach. Moreover, we state that the entanglement entropy approach is especially powerful in studying the effects of the dark matter sector in this general insulator/superconductor system.

PACS numbers: 11.25.Tq, 04.70.Bw, 74.20.-z

* yanpengphy@163.com
† panqiyuan@126.com
‡ liuyunqi@hust.edu.cn

I. INTRODUCTION

The anti-de Sitter/conformal field theories (AdS/CFT) correspondence relates the strongly correlated conformal field theory on the boundary with a weakly interacting gravity system in the bulk [1–3]. According to this novel idea, the gauge/gravity duality has been successfully employed to gain a better understanding of the low energy physics in condensed matter systems from a higher dimensional gravitational dual. The simplest holographic metal/superconductor model dual to gravity theories was constructed by applying a scalar field and a Maxwell field coupled in the AdS black hole background [4–6]. And then the holographic insulator/superconductor transiton was also established in the AdS soliton spacetime [7–9]. At present, a lot of more complete holographic superconductor models have been widely studied to model conductivity and other condensed matter physics properties in various gravity theories, such as the Einstein-Gauss-Bonnet gravity, Horava-Lifshitz gravity, non-linear electrodynamics gravity and so on, see Refs. [10]-[36].

Based on contemporary astrophysical observations, a new gravity theory with dark matter sector was recently established by introducing a new U(1) gauge field coupled to the normal Maxwell field [37, 38]. In order to construct more general holographic models, a holographic s-wave metal/superconductor model with dark matter sector was established in the AdS black hole background, for references see [39–41]. We have to confess that our universe is usually believed to be dS and the background here is AdS. But when studying holographic superconductors, one is normally interested in the conformal field theories on the boundary and thus the bulk AdS gravity with dark matter doesn't have to be realistic. In fact, it showed that the dark matter sector really provides richer physics in the critical temperature and also the stability of metal/superconductor transitions on the boundary. Most surprisingly, for a certain range of parameters, there is a novel phenomenon of retrograde condensation. The retrograde condensation was first introduced to describe the behavior of a binary mixture during isothermal compression above the critical temperature of the mixture [42]. On the side of holographic superconductor, this behaviors was already observed in Ref.[44] and the p-wave superconductor [43]. We further obtained the general conditions for retrograde condensations and proved retrograde condensations to be unstable in the s-wave metal/superconductor transitions [45]. It was also shown that the critical temperature is independent of the model parameter in the probe limit and when including backreaction, the lager model parameter corresponds to a smaller critical temperature or the condensation is more easier to happen. To the best of our knowledge, the effects of dark matter sector on the condensation in this model are

very different from properties of model parameters in other existing holographic models.

However, all the front holographic models with dark matter sector were constructed in the background of AdS black hole or describe metal/superconductor transitions. As a further step, the dark matter sector was also considered in the holographic insulator/superconductor transitions in the AdS soliton spacetime while neglecting the matter fields' backreaction on the metric [46, 47]. It was shown that the critical chemical potential is independent of the dark matter sector parameter without backreaction. In contrast, we will show in this work that the dark matter sector could affect the critical chemical potential and also the order of transitions when including backreaction. As we have described in the front paragraph, the dark matter sector could trigger retrograde condensation in the metal/superconductor model in the background of AdS black hole. Since the bulk AdS black hole gravity describes a metal/superconductor transition on the boundary and the AdS soliton background is dual to holographic insulator/superconductor transitions, we also plan to examine wether there is unstable retrograde condensation in the insulator/superconductor system due to the dark matter sector in the AdS soliton spacetime.

On the other hand, the entanglement entropy is usually applied to keep track of the degrees of freedom for strongly coupled system while other traditional methods might not be available. According to the AdS/CFT correspondence, it was proposed that the holographic entanglement entropy of a strongly interacting system on the boundary can be calculated from a weakly coupled gravity dual in the bulk [48, 49]. With this elegant approach, the holographic entanglement entropy has recently been used to study the properties of phase transitions in various holographic models and it provides us rich insights into the phase transitions [50]-[68]. For example, it was argued that the entanglement entropy is a good probe of the critical phase transition point and the order of phase transitions. Along this line, we would like to study the effects of the dark matter sector from the holographic entanglement entropy approach and examine whether the holographic entanglement entropy is still useful in disclosing properties of the dark matter sector in the general holographic insulator/superconductor model with backreaction.

This paper is organized as follows. In the next section, we introduce the holographic model with dark matter sector in the background of AdS soliton away from the probe limit. In part A of section III, we study the stability of holographic phase transitions. And in part B and part C of section III, we disclose properties of insulator/superconductor transitions by examining in detail behaviors of the scalar operator, the effective scalar mass and the holographic entanglement entropy of the system. We will summarize our main results in the last section.

II. EQUATIONS OF MOTION AND BOUNDARY CONDITIONS

In this work, we consider the holographic phase transitions with dark matter sector in the 5-dimensional AdS soliton spacetime. The general Lagrange density constructed by a scalar field and two U(1) gauge fields coupled in the gravitational background reads [39]

$$\mathcal{L} = R + \frac{12}{L^2} - \left(\frac{1}{4}F^{MN}F_{MN} + |\nabla_M\psi - iqA_M|^2 + m^2\psi^2 + \frac{1}{4}B^{MN}B_{MN} + \frac{\alpha}{4}B^{MN}F_{MN}\right), \tag{1}$$

where $\psi(r)$ is the complex scalar field, A_M stands for the ordinary Maxwell field and another additional $U(1)$ gauge field B_M corresponds to the dark matter field, which is not completely decoupled with the visible matter. $-6/L^2$ is the negative cosmological constant, where L is the radius of AdS spactime which will be scaled unity in the following numerical calculation. m is the mass of the scalar field, q is the scalar charge and α is the coupling parameter between the two U(1) gauge fields.

The Einstein equations for the system can be written in the form

$$R_{MN} - \frac{1}{2}g_{MN}R - 6g_{MN} = \frac{1}{2}\tilde{T}_{MN}, \tag{2}$$

where $\tilde{T}_{MN}$ is the energy-momentum tensor expressed as

$$\begin{aligned}\tilde{T}_{MN} &= F_{M\beta}F_N^{\beta} + B_{M\beta}B_N^{\beta} + \alpha B_{M\beta}F_N^{\beta} + 2\nabla_M\psi\nabla_N\psi + 2q^2A_MA_N\psi^2 \\ &+g_{MN}\left(-\frac{1}{4}F_{MN}F^{MN} - \frac{1}{4}B_{MN}B^{MN} - \frac{\alpha}{4}F_{MN}B^{MN} - \nabla_M\psi\nabla_M\psi - q^2A_MA^M\psi^2 - m^2\psi^2\right).\end{aligned} \tag{3}$$

With the variation of the considered matter fields, we obtain the corresponding independent equations of motion in the form

$$\nabla_M F^{MN} - 2q^2A^N\psi^2 + \frac{\alpha}{2}\nabla_M B^{MN} = 0, \tag{4}$$

$$\nabla_M\nabla^M\psi - q^2A_MA^M\psi - m^2\psi = 0, \tag{5}$$

$$\nabla_M B^{MN} + \frac{\alpha}{2}\nabla_M F^{MN} = 0. \tag{6}$$

Putting (6) into (4), we can eliminate the dark matter field and obtain the equation

$$\nabla_M F^{MN} - \frac{2q^2\psi^2A^N}{\tilde{\alpha}} = 0, \tag{7}$$

where $\tilde{\alpha} = 1 - \frac{\alpha^2}{4}$.

Substituting (7) into (6), we arrive at

$$\nabla_M B^{MN} + \frac{\alpha q^2\psi^2A^N}{\tilde{\alpha}} = 0. \tag{8}$$

For simplicity, we take the AdS soliton solutions and other matter fields in the forms

$$ds^2 = -r^2 e^{C(r)} dt^2 + \frac{dr^2}{r^2 B(r)} + r^2 dx^2 + r^2 dy^2 + r^2 B(r) e^{D(r)} d\chi^2, \tag{9}$$

$$A = \phi(r) dt, \qquad B = \eta(r) dt, \qquad \psi = \psi(r). \tag{10}$$

In order to get smooth solutions at the tip r_s satisfying $B(r_s) = 0$, we have to impose on the coordinate χ a period Γ as

$$\Gamma = \frac{4\pi e^{-D(r_s)/2}}{r_s^2 B'(r_s)}. \tag{11}$$

We also need $C(r \to \infty) = 0$ and $D(r \to \infty) = 0$ to recover the AdS boundary.

From above assumptions, we can obtain the equations of motion as

$$\psi'' + \left(\frac{5}{r} + \frac{B'}{B} + \frac{C'}{2} + \frac{D'}{2}\right)\psi' + \frac{q^2 \phi^2 e^{-C}}{r^4 B}\psi - \frac{m^2}{r^2 B}\psi = 0, \tag{12}$$

$$\phi'' + \left(\frac{3}{r} + \frac{B'}{B} - \frac{C'}{2} + \frac{D'}{2}\right)\phi' - \frac{2q^2 \psi^2}{\tilde{\alpha} r^2 B}\phi = 0, \tag{13}$$

$$\eta'' + \left(\frac{3}{r} + \frac{B'}{B} - \frac{C'}{2} + \frac{D'}{2}\right)\eta' + \frac{\alpha q^2 \psi^2 \phi}{\tilde{\alpha} r^2 B} = 0, \tag{14}$$

$$C'' + \frac{1}{2}C'^2 + \left(\frac{5}{r} + \frac{A'}{2} + \frac{B'}{B}\right)C' - \frac{e^{-C}}{r^2}\left(\phi'^2 + \eta'^2 + \alpha\phi'\eta'\right) - \frac{2q^2\phi^2\psi^2 e^{-C}}{r^4 B} = 0, \tag{15}$$

$$B'\left(\frac{3}{r} - \frac{C'}{2}\right) + B\left[\psi'^2 - \frac{1}{2}A'C' + \frac{e^{-C}}{2r^2}\left(\phi'^2 + \eta'^2 + \alpha\phi'\eta'\right) + \frac{12}{r^2}\right] + \frac{q^2\phi^2\psi^2 e^{-C}}{r^4} + \frac{m^2\psi^2}{r^2} - \frac{12}{r^2} = 0, \tag{16}$$

$$D' = \frac{2r^2 C'' + r^2 C'^2 + 4rC' - 2e^{-C}(\phi'^2 + \eta'^2 + \alpha\phi'\eta') + 4r^2\psi'^2}{r(6 + rC')}, \tag{17}$$

where the prime denotes the derivative with respect to r. Since the equations are nonlinear and coupled to each other, we have to solve these equations by using the numerical shooting method which will integrate the equations of motion from the tip of the soliton out to the infinity. Thus, we have to specify the boundary conditions for this system. At the tip, we can impose proper boundary conditions as

$$\begin{aligned}
&\psi(r) = \psi_0 + \psi_1(r - r_s) + \cdots, \quad \phi(r) = \phi_0 + \phi_1(r - r_s) + \cdots, \\
&\eta(r) = \eta_0 + \eta_1(r - r_s) + \cdots, \quad B(r) = B_0(r - r_s) + B_1(r - r_s)^2 + \cdots, \\
&C(r) = C_0 + C_1(r - r_s) + \cdots, \quad D(r) = D_0 + D_1(r - r_s) + \cdots,
\end{aligned} \tag{18}$$

where the dots denote higher order terms. In view of the equations of motion, we are left with six independent parameters r_s, ψ_0, ϕ_0, η_0, C_0 and D_0 at the tip. Near the AdS boundary ($r \to \infty$), the asymptotic behaviors of the solutions are

$$\begin{aligned} &\psi \to \frac{\psi_-}{r^{\lambda_-}} + \frac{\psi_+}{r^{\lambda_+}} + \cdots, \quad \phi \to \mu - \frac{\rho}{r^2} + \cdots, \quad \eta \to \xi - \frac{\varpi}{r^2} + \cdots, \\ &B \to 1 + \frac{B_4}{r^4} + \cdots, \quad C \to \frac{C_4}{r^4} + \cdots, \quad D \to \frac{D_4}{r^4} + \cdots, \end{aligned} \tag{19}$$

with $\lambda_\pm = (2 \pm \sqrt{4+m^2})$. μ and ρ can be interpreted as the chemical potential and charge density in the dual theory respectively. The other two operators ξ and ϖ are dual to the U(1) gauge field $\eta(r)$.

From the equations of motion for the system, we obtain the scaling symmetry

$$r \to ar, \qquad (\chi, x, y, t) \to (\chi, x, y, t)/a, \qquad \phi \to a\phi, \qquad \eta \to a\eta, \tag{20}$$

which can be used to set $r_s = 1$ in the following calculation. Choosing $m^2 = -2 > -\frac{9}{4}$ above the BF bound [69], the second mode ψ_+ is always normalizable. To get a stable theory, we will fix $\psi_- = 0$ and use the operator $\psi_+ =< O_+ >$ to describe the phase transition in the dual CFT. For different values of ψ_0, we can rely on the independent parameters ϕ_0, η_0, C_0 and D_0 as the shooting parameter to search for the solutions with the boundary conditions $\psi_- = 0$, $C(r \to \infty) = 0$, $D(r \to \infty) = 0$ and $\frac{\xi}{\mu}$ fixed.

III. HOLOGRAPHIC PHASE TRANSITIONS IN ADS SOLITON BACKGROUND

A. Stability of the phase transitions

In this part, we investigate the stability of holographic insulator/superconductor phase transitions through the behaviors of the scalar operator. We choose the example $\Gamma = \pi$, $m^2 = -2$, $q = 2$, $\alpha = 2.5$ and $\frac{\xi}{\mu} = -1$ in Fig. 1. It is surprising in the left panel that the condensed phases appears at small chemical potential $\mu < \mu_c = 0.944$, which is different from the normal results in [7, 9]. We refer this phenomenon as the retrograde condensation, which was also observed in the holographic metal/superconductor transitions in the background of AdS black hole [39, 45]. By choosing different sets of parameters, we find that there are retrograde condensations for all superconducting solutions satisfying $\frac{\xi}{\mu} = -1$ and $\alpha > 2$.

In order to determine whether the retrograde condensation is thermodynamically favored, we should calculate the free energy of the system for both normal phase and condensed phase. We show the corresponding free energy of the system in the right panel of Fig. 1. It shows that the free energy of this hairy AdS soliton is larger than the free energy of the soliton in normal phase. Since the physical procedure corresponds to the

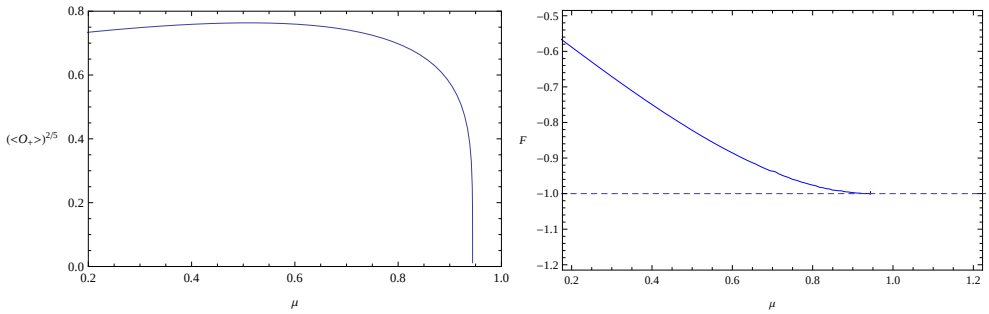

FIG. 1: (Color online) The phase transition in cases of $\Gamma = \pi$, $m^2 = -2$, $q = 2$, $\alpha = 2.5$ and $\frac{\xi}{\mu} = -1$. The left panel shows the behavior of the scalar condensation. The right panel represents the free energy of the system, where the solid line corresponds to the superconducting phase and the dashed line is with the normal phase.

phases with the lowest free energy, we arrive at a conclusion that the retrograde condensation superconducting solutions are thermodynamically unstable and the unusual behaviors of the scalar operator can be used to detect the thermodynamical instability of phase transitions.

Now we study the case of $\Gamma = \pi$, $m^2 = -2$, $q = 2$, $\alpha = 0.5$ and $\frac{\xi}{\mu} = 1$ in Fig. 2. In the left panel, we find a critical chemical potential $\mu_c = 0.944$ above which there is scalar condensation. In order to further study the phase transition, we plot the free energy in the right panel of Fig. 2. The free energy of superconducting state lies below the free energy of the normal state, which suggests that the superconducting solutions are thermodynamically stable. More calculations show that phase transitions are thermodynamically stable for all $\alpha > 0$ and $\frac{\xi}{\mu} = 1$. When $\frac{\xi}{\mu} = -1$, there are thermodynamically stable solutions for $0 \leqslant \alpha < 2$.

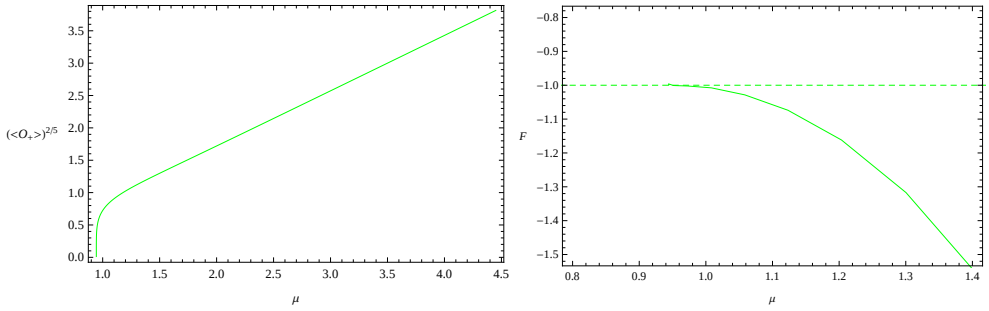

FIG. 2: (Color online) The phase transitions in cases of $\Gamma = \pi$, $m^2 = -2$, $q = 2$, $\alpha = 0.5$ and $\frac{\xi}{\mu} = 1$. The left panel represents the scalar operator with respect to the chemical potential. The solid line in the right panel shows the free energy of the superconducting phase and the dashed line corresponds to normal phases.

With fitting methods, we obtain approximate formulas for the free energy of normal state (F_{SL}) and superconducting state (F_{SC}) that:

$$F_{SL} \approx -1.00, \qquad F_{SC} \approx -1.00 - 2.21(\mu - \mu_c)^2 - 0.86(\mu - \mu_c)^3. \tag{21}$$

The front formulas suggest that: $F_{SL}|_{\mu=\mu_c} = F_{SC}|_{\mu=\mu_c}$, $\frac{\partial F_{SL}}{\partial \mu}|_{\mu=\mu_c} = \frac{\partial F_{SC}}{\partial \mu}|_{\mu=\mu_c}$, $\frac{\partial^2 F_{SL}}{\partial \mu^2}|_{\mu=\mu_c} \neq \frac{\partial^2 F_{SC}}{\partial \mu^2}|_{\mu=\mu_c}$. In other words, the curve representing the physical phases with the lowest free energy is smooth at the critical

point μ_c or the insulator/superconductor transition is of the second order.

B. Properties of the scalar condensation with $q = 2$

For simplicity, we fix $\frac{\xi}{\mu} = 1$ and focus on the stable transitions in the following discussion. We show the scalar operator $\langle O_+ \rangle^{1/\lambda_+}$ as a function of μ with $\Gamma = \pi$, $m^2 = -2$ and $q = 2$ in Fig. 3. It is shown that there are phase transitions at critical chemical potentials, above which the charged scalar condensation turns on. We exhibit the condensation of the scalar operator by choosing various α from top to bottom as: $\alpha = 0$, $\alpha = 0.5$, $\alpha = 1.0$ and $\frac{\xi}{\mu} = 1$. The increase of the parameter α develops shallower condensation gap. And in both curves, the critical chemical potential keeps as a constant $\mu_c = 0.944$ for different values of α. In all, the effects of the dark matter sector on the critical phase transition points and condensation gap are very different from those reported in the metal/superconductor system [39, 40, 45]. We conclude that the effects of the dark matter sector on transitions depend on backgrounds.

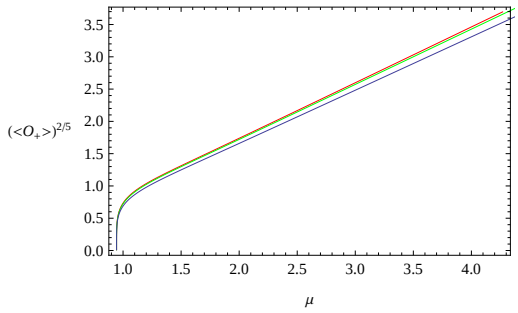

FIG. 3: (Color online) The phase transition in the cases of $\Gamma = \pi$, $m^2 = -2$ and $q = 2$. It shows the behavior of scalar operator with $\frac{\xi}{\mu} = 1$ and various α from top to bottom as: $\alpha = 0$ (red), $\alpha = 0.5$ (green)and $\alpha = 1$ (blue).

From another aspect, the negative effective mass is crucial to cause the condensation of scalar fields [27]. We can disclose the effects of α on the phase transitions through the effective scalar mass. When including backreaction, the effective mass of the scalar field is expressed as

$$m_{eff}^2 = m^2 + g^{tt} A_{tt}^2 = -2 - \frac{\phi^2}{r^2 e^C}. \tag{22}$$

We plot the effective scalar mass as a function of $z = \frac{1}{r}$ with $r_s = 1$, $m^2 = -2$, $q = 2$ and $< O_+ >= 1.0$ in Fig. 4. The lines from bottom to top correspond to the increase of α as: $\alpha = 0$, $\alpha = 0.5$ and $\alpha = 1$ with $\frac{\xi}{\mu} = 1$. It can be easily seen from the picture that a larger α will lead the effective mass to develop shallower and narrower wells out of the tip, which corresponds to a lower gap of condensation for the operator. Thus, we arrive at the same conclusion just as shown in Fig. 3 that the larger parameter α leads to a lower gap of condensation.

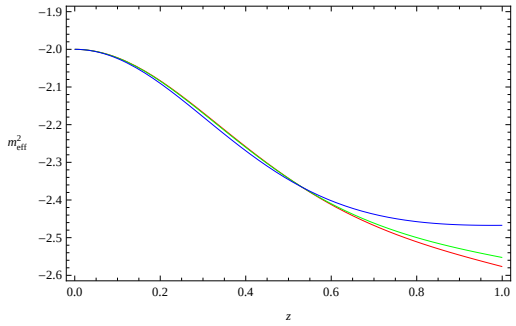

FIG. 4: (Color online) The phase transition in the cases of $\Gamma = \pi$, $m^2 = -2$ and $q = 2$. It shows the behaviors of effective mass with $\frac{\xi}{\mu} = 1$ and various α from bottom to top as: $\alpha = 0$ (red), $\alpha = 0.5$ (green), $\alpha = 1$ (blue).

In the following, we pay attention to the holographic entanglement entropy(HEE) of the transition system. The authors in Refs. [48, 49] have provided a method to compute the entanglement entropy of conformal field theories (CFTs) from the gravity side. For simplicity, we consider the entanglement entropy for a half space corresponding to a subsystem $\bar{A}$ defined by $x > 0$, $-\frac{R}{2} < y < \frac{R}{2}$ $(R \to \infty)$, $0 \leqslant \chi \leqslant \Gamma$. Then the entanglement entropy can be expressed as [60–62]:

$$S_{\bar{A}}^{half} = \frac{R\Gamma}{4G_N}\int_{r_0}^{\frac{1}{\varepsilon}} re^{\frac{D(r)}{2}}dr = \frac{R\pi}{8G_N}(\frac{1}{\varepsilon^2} + S), \tag{23}$$

where $r = \frac{1}{\varepsilon}$ is the UV cutoff. The first term is divergent as $\varepsilon \to 0$. In contrast, the second term does not depend on the cutoff and thus is physical important. As a matter of fact, this finite term is the difference between the entanglement entropy in the pure AdS soliton and the pure AdS space. $S = -1$ corresponds to the pure AdS soliton.

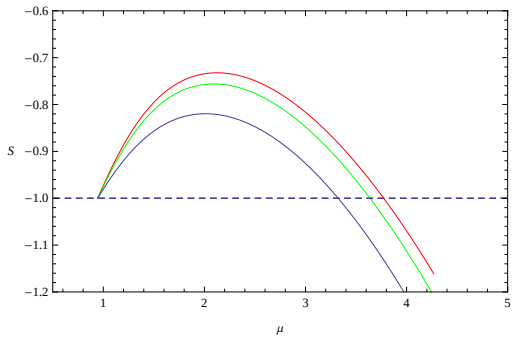

FIG. 5: (Color online) The holographic entanglement entropy as a function of the chemical potential μ for $\Gamma = \pi$, $m^2 = -2$ and $q = 2$. The dashed lines correspond to the entanglement entropy of a pure AdS soliton and the solid lines correspond to cases of superconducting solutions. We have choose $\frac{\xi}{\mu} = 1$ and various α from top to bottom as: $\alpha = 0$ (red), $\alpha = 0.5$ (green) and $\alpha = 1.0$ (blue).

We present the holographic entanglement entropy as a function of the chemical potential μ in Fig. 5 with $\Gamma = \pi$, $m^2 = -2$, $q = 2$, $\frac{\xi}{\mu} = 1$ and with various α. For all set of parameters, we find a threshold chemical

potential $\mu = 0.944$, above which the hairy soliton appears. The jump of the slop of the entanglement entropy at $\mu = 0.944$ signals that some kind of new degrees of freedom like the Cooper pair would emerge in the new phase. It also can be easily seen from the pictures that when the parameters are fixed, the entanglement entropy first increases and then decreases monotonously as we choose a larger chemical potential. It means that there is firstly a increase and then a reduction in the number of degrees of freedom due to the condensate generated in the phase transitions [65]. Considering that deeper condensates with larger entanglement entropy around the phase transition point, again it can be concluded from Fig. 5 that larger α corresponds to a smaller scalar operator around the phase transition point. We also see that larger α corresponds to smaller maximum entanglement entropy. Then it is an interesting question whether the entanglement entropy will decrease similar to the case in AdS black hole when we choose a very large α. Most importantly, we mention that the entanglement entropy is more sensitive to the change of the coupling parameter α than the scalar operator and effective mass, which proves the entanglement entropy to be a powerful approach to detect the effects of the dark matter sector.

The critical phase transition point $\mu = 0.944$ obtained from the behaviors of holographic entanglement entropy is equal to the threshold chemical potential $\mu_c = 0.944$ obtained from the behaviors of the free energy and the scalar operator. That means the holographic entanglement entropy can be used to search for the critical phase transition points. And the jump of the slope of holographic entanglement entropy corresponds to second order phase transitions in the general holographic superconductor model with dark matter sector. In summary, we conclude that the entanglement entropy can be used to determine the critical phase transition point, the order of the phase transition and the values of the coupling parameter α. So the entanglement entropy is indeed a good probe of insulator/superconductor phase transitions with dark matter sector.

C. Various phase transitions with $q = 1$

Now we pay attention to the holographic superconductor with small charge $q = 1$. We exhibit the free energy as a function of the chemical potential in Fig. 6 with $\Gamma = \pi$, $m^2 = -2$ and various α. It can be seen from the left panel that, for the small model parameter $\alpha = 0.1$, F develops a discontinuity in the first derivative of the free energy with respect to the chemical potential at a critical value $\mu_c = 1.82$, which implies the first order phase transition. In the middle panel with $\alpha = 1.0$, F decreases smoothly near the critical point $\mu_c = 1.89$ indicating the second order phase transitions from normal state into superconducting state. What's more, besides the second order phase transition at $\mu_c = 1.89$, the free energy develops a "swallow tail" at $\mu = 2.08$

within the superconducting phase, a typical signal for a first order phase transition. The right panel shows that when the coupling parameter is larger as $\alpha = 1.5$, there is only second order insulator/superconductor phase transitions at the critical phase transition point $\mu_c = 1.89$. We conclude that the dark matter sector can affect the critical phase transition points and also the order of phase transitions.

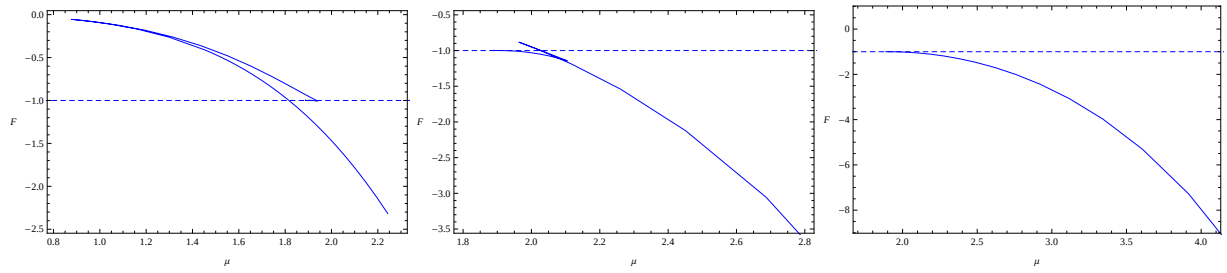

FIG. 6: (Color online) The free energy with respect to the chemical potential in cases of $\Gamma = \pi$, $m^2 = -2$, $q = 1$ and $\frac{\xi}{\mu} = 1$. The panels from left to right represent the cases of $\alpha = 0.1$, $\alpha = 1.0$ and $\alpha = 1.5$. The solid line corresponds to the superconducting phase and the dashed line of $S = -1$ is with the normal phase.

We also detect the properties of phase transitions by studying the corresponding behaviors of the scalar operator in Fig. 7. In the left panel with $\alpha = 0.1$, at the critical chemical potential $\mu_c = 1.82$, the scalar operator $\langle O_+ \rangle^{1/\lambda_+}$ has a jump from insulator state to superconductor state indicating a first order phase transition. When choosing $\alpha = 1.0$ in the middle panel, the curves firstly increase continuously around the insulator/superconductor points $\mu_c = 1.89$ and then have a jump at $\mu = 2.08$ in the superconducting state. It means there are second order phase transitions at $\mu_c = 1.89$ and then first order phase transitions at $\mu = 2.08$. In cases of lager parameter $\alpha = 1.5$ in the right panel, $\langle O_+ \rangle^{1/\lambda_+}$ increases continuously with chemical potential, which is a classical performance of the second order phase transition.

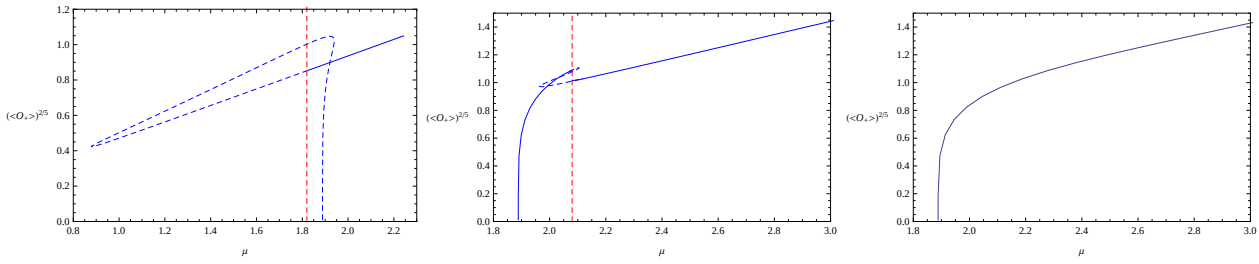

FIG. 7: (Color online) The behaviors of scalar operator in cases of $\Gamma = \pi$, $m^2 = -2$, $q = 1$ and $\frac{\xi}{\mu} = 1$. The panels from left to right show the case of $\alpha = 0.1$, $\alpha = 1.0$ and $\alpha = 1.5$. The blue solid lines correspond to the physical superconducting states

At last, we turn to study the holographic phase transition through the entanglement entropy approach. We plot the corresponding entanglement entropy with respect to the chemical potential μ in Fig. 8 with $\alpha = 1.0$. The blue dashed line $S = -1$ describes the entanglement entropy of the normal phase, while the blue solid line correspond to the entanglement entropy of the superconducting phase. The holographic entanglement

entropy is continuously at the critical chemical potential $\mu = 1.89$ and there are discontinuous slops at this transition point, which implies the phase transitions at $\mu = 1.89$ are of the second order. When we go on to increase the chemical potential, the entanglement entropy has a jump around $\mu = 2.08$ which corresponds to the "swallow tail" of the free energy F in Fig. 6 and the dump of the scalar operator in Fig. 7. The front phenomenon implies a first order phase transition around $\mu = 2.08$ in the superconducting phase. We state that the entanglement entropy can be used to study the critical phase transition points and the order of phase transitions in our general holographic superconductor model.

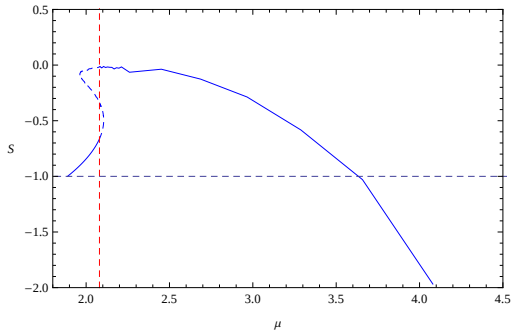

FIG. 8: (Color online) The the entanglement entropy in cases of $\Gamma = \pi$, $m^2 = -2$, $q = 1$, $\alpha = 1.0$ and $\frac{\xi}{\mu} = 1$. The blue solid line shows the the entanglement entropy of the superconducting phase and the blue dashed line $S = -1$ corresponds to normal phases.

IV. CONCLUSIONS

We generalize holographic insulator/superconductor transition model in the presence of dark matter sector by including backreaction. In the previous model without backreaction, the scalar charge q can be scaled unity without loss of generality. While including backreaction in this work, we treat the scalar charge q as a parameter and obtain much more richer physics by choosing various q. We disclosed properties of transitions through analyzing behaviors of the scalar operator, the effective scalar mass, and also the holographic entanglement entropy of the system. Firstly, we observe unstable phases refered as retrograde condensation due to the dark matter sector and also obtained the stability conditions. For the large scalar charge q, it was shown that the phase transition is of the second order and the larger coupling parameter α makes the gap of condensation lower. And the critical phase transition chemical potential is always a constant for different values of α similar to cases without backreaction. When we choose very small charge q, the parameter α could affect the critical chemical potential and the order of phase transitions, which is very different from cases in the probe limit. These conclusions can also be well understood from the behaviors of the holographic topological entanglement entropy of the system. Moreover, we pointed out that the entanglement entropy is more

sensitive to the change of the coupling parameter α than the scalar operator and effective mass. In summary, we found that the dark matter sector provides much more richer physics when including backreaction.

Acknowledgments

This work was supported by the National Natural Science Foundation of China under Grant Nos. 11305097, 11275066 and 11505066; the Shaanxi Province Science and Technology Department Foundation of China under Grant No. 2016JQ1039. This work was also partly finished during the International Conference on holographic duality for condensed matter physics at Kavli Institute for Theoretical Physics China (KITPC), Chinese Academy of Sciences on July 6-31, 2015.

[1] J.M. Maldacena,The large-N limit of superconformal field theories and supergravity, Adv. Theor. Math. Phys. **2**, 231 (1998).
[2] S.S. Gubser, I.R. Klebanov, and A.M. Polyakov,Gauge theory correlators from non-critical string theory, Phys. Lett. B **428**, 105 (1998).
[3] E. Witten,Anti-de Sitter space and holography, Adv. Theor. Math. Phys. **2**, 253 (1998).
[4] S.A. Hartnoll,Lectures on holographic methods for condensed matter physics, Class. Quant. Grav. **26**, 224002 (2009).
[5] C.P. Herzog,Lectures on Holographic Superfluidity and Superconductivity, J. Phys. A **42**, 343001 (2009).
[6] G.T. Horowitz,Introduction to Holographic Superconductors, Lect. Notes Phys. **828** 313, (2011); arXiv:1002.1722 [hep-th].
[7] T. Nishioka, S. Ryu and T. Takayanagi, Holographic Superconductor/Insulator Transition at Zero Temperature, JHEP 03 (2010) 131 [arXiv:0911.0962] [INSPIRE].
[8] G.T. Horowitz and B. Way, Complete Phase Diagrams for a Holographic Superconductor/Insulator System, JHEP 11 (2010) 011 [arXiv:1007.3714] [INSPIRE].
[9] Y. Peng, Q. Pan and B. Wang, Various types of phase transitions in the AdS soliton background, Phys. Lett. B 699 (2011) 383 [arXiv:1104.2478] [INSPIRE].
[10] R.Gregory, S.Kanno, and J.Soda, JHEP 10, 010 (2009).
[11] L.Barclay, R.Gregory, S.Kanno, and P.Sutcliffe, JHEP 12, 029 (2010).
[12] Q.Pan, B.Wang, E.Papantonopoulos, J.Oliviera, and A.Pavan, Phys. Rev. D 81, 106007 (2010).
[13] F.Aprile and J.G.Russo, Phys. Rev. D 81, 026009 (2010).
[14] A.Salvio, Holographic superfluids and superconductors in dilaton gravity, hep-th 1207.3800 (2012).
[15] R.Cai and H.Zhang, Phys. Rev. D 81, 066003 (2010).
[16] J.Jing, Q.Pan, and S.Chen, JHEP 11, 05 (2011)
[17] G.T. Horowitz and M.M. Roberts, Phys. Rev. D **78**, 126008 (2008).
[18] J. Sonner, A Rotating Holographic Superconductor, Phys. Rev. D **80**, 084031 (2009).
[19] Qiyuan Pan, Bin Wang, General holographic superconductor models with backreactions, arXiv:1101.0222v1.
[20] S.A. Hartnoll, C.P. Herzog and G.T. Horowitz,Holographic Superconductors, J. High Energy Phys. **0812**, 015 (2008)
[21] Y.Q. Liu, Q.Y. Pan, and B. Wang,Holographic superconductor developed in BTZ black hole background with backreactions, Phys. Lett. B **702**, 94 (2011).
[22] Y.Peng, X.M. Kuang, Y.Q. Liu, and B. Wang, Phase transition in the holographic model of superfluidity with backreactions, arXiv:1106.4353 [hep-th].
[23] J.P. Gauntlett, J. Sonner, and T. Wiseman,Holographic superconductivity in M-Theory, Phys. Rev. Lett. **103**, 151601 (2009).
[24] J.L. Jing and S.B. Chen, Holographic superconductors in the Born-Infeld electrodynamics,Phys. Lett. B **686**, 68 (2010).
[25] K. Maeda, M. Natsuume, and T. Okamura,Universality class of holographic superconductors, Phys. Rev. D **79**, 126004 (2009).
[26] X.H. Ge, B. Wang, S.F. Wu, and G.H. Yang, Analytical study on holographic superconductors in external magnetic field, J. High Energy Phys. **1008**, 108 (2010).
[27] Y. Brihaye and B. Hartmann, Holographic superconductors in 3 + 1 dimensions away from the probe limit, Phys. Rev. D **81**, 126008 (2010).

[28] C. P. Herzog, P. K. Kovtun, D. T. Son, Holographic model of superfluidity, Phys. Rev. D **79**, 066002.
[29] G.T. Horowitz and B. Way, Complete Phase Diagrams for a Holographic Superconductor/Insulator System, J. High Energy Phys. **1011**, 011 (2010).
[30] Dibakar Roychowdhury, AdS/CFT superconductors with Power Maxwell electrodynamics: reminiscent of the Meissner effect, Physics Letters B 718 (2013).
[31] S. Franco, A.M. Garcia-Garcia, and D. Rodriguez-Gomez, A general class of holographic superconductors, J. High Energy Phys. **1004**, 092 (2010).
[32] S. Franco, A.M. Garcia-Garcia, and D. Rodriguez-Gomez, A holographic approach to phase transitions, Phys. Rev. D **81**, 041901(R) (2010).
[33] Q.Y. Pan and B. Wang, General holographic superconductor models with Gauss-Bonnet corrections, Phys. Lett. B **693**, 159 (2010).
[34] Y. Peng, and Q.Y. Pan, St*ü*ckelberg Holographic Superconductor Models with Backreactions,Commun. Theor. Phys. **59**, 110 (2013).
[35] Daniel Arean, Leopoldo A. Pando Zayas, Ignacio Salazar Landea, Antonello Scardicchio, The Holographic Disorder-Driven Supeconductor-Metal Transition, arXiv:1507.02280 [hep-th]
[36] Matteo Baggioli, Mikhail Goykhman, Phases of holographic superconductors with broken translational symmetry, JHEP07(2015)035.
[37] H.Davoudiasl, H.-S.Lee, I.Lewis, and W.J.Marciano, Phys. Rev. D 85, 115019 (2012), ibid. 88, 015022 (2013), C.-F Chang, E.Ma, and T.-C.Yuan, Multilepton Higgs Deacays through the Dark Portal, hep-ph 1308.6071 (2014).
[38] T.Vachaspati and A.Achucarro, Phys. Reports 327, 347 (2000), T.Vachaspati, Dark Strings, hep-th 0902.1764 (2009), B.Hartmann and F.Arbabzadah, JHEP 07, 068 (2009), Y.Brihaye and B.Hartmann, Phys. Rev. D 80, 123502 (2009).
[39] Lukasz Nakonieczny and Marek Rogatko, Analytic study on backreacting holographic superconductors with dark matter sector, Phys.Rev.D90, 106004 (2014).
[40] Lukasz Nakonieczny, Marek Rogatko and Karol I. Wysokinski, Magnetic field in holographic superconductor with dark matter sector, Phys.Rev.D91, 046007 (2015).
[41] Marek Rogatko and Karol I. Wysokinski, Holographic vortices in the presence of dark matter sector, arXiv:1510.06137.
[42] J. P. Kuenen, Measurements on the surface of Van der Waals for mixtures of carbonic acid and methyl chloride, Commun. Phys. Lab. Univ. Leiden, No 4 (1892).
[43] Rong-Gen Cai, Li Li, Li-Fang Li, A Holographic P-wave Superconductor Model,JHEP 1401 (2014) 032.
[44] F.Aprile, D.Roest, and J.G.Russo, JHEP 06, 040 (2011).
[45] Yan Peng, Holographic entanglement entropy in superconductor phase transition with dark matter sector, Physics Letters B 750 (2015).
[46] Marek Rogatko Karol I. Wysokinski, P-wave holographic superconductor/insulator phase transitions affected by dark matter sector, arXiv:1508.02869v1.
[47] Lukasz Nakonieczny, Marek Rogatko and Karol I. Wysoki*ń*ski, Analytic investigation of holographic phase transitions influenced by dark matter sector, arXiv:1509.01769v1.
[48] S. Ryu and T. Takayanagi, Holographic Derivation of Entanglement Entropy from AdS/CFT, Phys. Rev. Lett. **96**, 181602 (2006).
[49] S. Ryu and T. Takayanagi, Aspects of Holographic Entanglement Entropy, J. High Energy Phys. **0608**, 045 (2006).
[50] T. Nishioka and T. Takayanagi, Entropy and Closed String Tachyons, J. High Energy Phys. **0701**, 090 (2007).
[51] I.R. Klebanov, D. Kutasov, and A. Murugan, Entanglement as a Probe of Confinement, Nucl. Phys. B **796**, 274 (2008).
[52] A. Pakman and A. Parnachev, Topological Entanglement Entropy and Holography, J. High Energy Phys. **0807**, 097 (2008).
[53] T. Nishioka, S. Ryu, and T. Takayanagi, Holographic Entanglement Entropy: An Overview, J. Phys. A **42**, 504008 (2009).
[54] L.-Y. Hung, R.C. Myers, and M. Smolkin, On Holographic Entanglement Entropy and Higher Curvature Gravity, J. High Energy Phys. **1104**, 025 (2011).
[55] J. de Boer, M. Kulaxizi, and A. Parnachev,Holographic Entanglement Entropy in Lovelock Gravities, J. High Energy Phys. **1107**, 109 (2011).
[56] N. Ogawa and T. Takayanagi, Higher Derivative Corrections to Holographic Entanglement Entropy for AdS Solitons, J. High Energy Phys. **1110**, 147 (2011).
[57] T. Albash and C.V. Johnson, Holographic Entanglement Entropy and Renormalization Group Flow, J. High Energy Phys. **1202**, 095 (2012).
[58] R.C. Myers and A. Singh, Comments on Holographic Entanglement Entropy and RG Flows, J. High Energy Phys. **1204**, 122 (2012).
[59] X.M. Kuang, E. Papantonopoulos, and B. Wang, Entanglement Entropy as a Probe to the Proximity Effect in Holographic Superconductors, arXiv:1401.5720 [hep-th].
[60] R.-G. Cai, S. He, L. Li and Y.-L. Zhang, Holographic Entanglement Entropy in Insulator/Superconductor Transition, JHEP 07 (2012) 088 [arXiv:1203.6620] [INSPIRE].
[61] R.-G. Cai, S. He, L. Li and L.-F. Li, Entanglement Entropy and Wilson Loop in Stuckelberg Holographic Insulator/Superconductor Model, JHEP 10 (2012) 107 [arXiv:1209.1019] [INSPIRE].

[62] Weiping Yao, Jiliang Jing, Holographic entanglement entropy in metal/superconductor phase transition with Born-Infeld electrodynamics, arXiv:1408.1171 [hep-th].
[63] T. Albash and C.V. Johnson, Holographic Studies of Entanglement Entropy in Superconductors, J. High Energy Phys. **1205**, 079 (2012); arXiv:1202.2605 [hep-th].
[64] B. Swingle and T. Senthil, Universal crossovers between entanglement entropy and thermal entropy, arXiv:1112.1069 [cond-mat.str-el].
[65] R.-G. Cai, S.He, L.Li and Y.-L.Zhang, Holographic Entanglement Entropy on P-wave Superconductor Phase Tansition, JHEP 07(2012)027.
[66] L.-F. Li, R.-G. Cai, L.Li and C. Shen, Entanglement Entropy in a holographic P-wave Superconductor model, arXiv:1310.6239.
[67] Yan Peng, Qiyuan Pan, Holographic entanglement entropy in general holographic superconductor models,JHEP 06(2014)011.
[68] Yan Peng and Yunqi Liu, A general holographic metal/superconductor phase transition model, JHEP02(2015)082.
[69] P. Breitenlohner and D.Z. Freedman, Positive energy in Anti-de Sitter backgrounds and gauged extended supergravity, Phys. Lett. B **115**, 197 (1982).